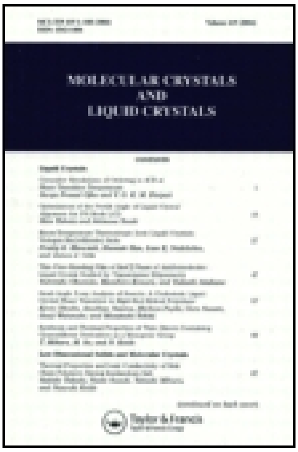

Molecular Crystals and Liquid Crystals
Publication details, including instructions for authors and subscription information:
http://www.tandfonline.com/loi/gmcl20

Monte-Carlo Simulations for Model Bent-Core Molecules with Fluctuating Opening Angle

W. Józefowicz [a] [b] & L. Longa [b]

[a] Department of Chemistry, University of York, Heslington, York, United Kingdom

[b] Department of Statistical Physics and Mark Kac Center for Complex Systems Research, Marian Smoluchowski Institute of Physics, Jagellonian University, Kraków, Poland

Version of record first published: 30 Jun 2011

To cite this article: W. Józefowicz & L. Longa (2011): Monte-Carlo Simulations for Model Bent-Core Molecules with Fluctuating Opening Angle, Molecular Crystals and Liquid Crystals, 545:1, 204/[1428]-213/[1437]

To link to this article: http://dx.doi.org/10.1080/15421406.2011.572014

Mol. Cryst. Liq. Cryst., Vol. 545: pp. 204/[1428]–213/[1437], 2011

ISSN: 1542-1406 print/1563-5287 online
DOI: 10.1080/15421406.2011.572014

Monte-Carlo Simulations for Model Bent-Core Molecules with Fluctuating Opening Angle

W. JÓZEFOWICZ[1,2] AND L. LONGA[2]

[1]Department of Chemistry, University of York, Heslington, York, United Kingdom
[2]Department of Statistical Physics and Mark Kac Center for Complex Systems Research, Marian Smoluchowski Institute of Physics, Jagellonian University, Kraków, Poland

We study the effect of fluctuations in opening angle of bent-core molecules on stability of the nematic phases. The molecules are built out of two Gay-Berne centers each corresponding to one of the molecular arms. Constant-pressure Monte Carlo (MC NPT) simulations are carried out for two versions of the model, with fixed- and fluctuating opening angle, where fluctuations are taken harmonic about the angle of 140°. The phases found on cooling are uniaxial nematic, biaxial nematic and crystalline. On heating the biaxial nematic is superseded by the metastable crystalline phase.

Keywords Banana-shaped molecules; biaxial nematic phase; NPT Monte Carlo simulation

1. Introduction

The most common phases found for bent-core liquid crystals are smectics [1]. It has therefore been quite surprising to discover that these systems can also stabilize the thermotropic uniaxial (N_U)- and biaxial nematic (N_B) phases [2–5], with quest for N_B occupying soft matter research for more than 30 years now (*see e.g.,*[6]). To date the factors crucial for absolute stability of the N_B phase in bent-core systems are not fully understood. In this work we carry out MC NPT simulations for model bent-core (V-shaped) molecules to seek for the *minimal molecular features* necessary to stabilize N_B. An excellent recent review on theoretical- and computer simulation attempts to find the N_B phase in model systems is found in [7]. A brief summary of the results relevant for what follows is given below.

The lattice simulations with *'bent-core'* dispersion centers occupying lattice sites of a cubic lattice show that the N_B phase can be stabilized about the Landau point at, or close to, the 'tetrahedral' opening angle of $cos^{-1}(-1/3) = 109.47°$ [8–10]. Additional inclusion of the dipole-dipole interactions with dipole moments along the C_2 molecular axis can transform the Landau point into a Landau line [10].

Address correspondence to L. Longa, Department of Statistical Physics and Mark Kac Center for Complex Systems Research, Marian Smoluchowski Institute of Physics, Jagellonian University, Reymonta 4, 30-059 Kraków, Poland. Tel.: +48-12663 5667; Fax: +48-126337; E-mail: lech.longa@uj.edu.pl

The presently existing simulations for model bent-core mesogens with centers of mass free to move (off-lattice) are less optimistic. The excluded volume effects (packing entropy) make the stable nematic phases, especially the biaxial one, rare to appear in these systems. For example, an ensemble of bend-core molecules formed by two rigid spherocylinders joined at one end stabilize only N_U and isotropic fluid [11,12]. Replacing spherocylinders with Gay-Berne (GB) centers of $\kappa = 3$, $\kappa' = 5$ also does not bring a stable biaxial nematic, as shown by Memmer [13] and Johnston *et al.* [14,15]. Even the N_U phase disappears for an intermediate opening angle of 110°. Similar conclusions as concerning stability of N_U can be drawn from NPT MC simulations of Dewar and Camp [16] for the multi-site bent-core model of rigidly connected LJ spherical sites.Before proceeding further we would like to mention about an interesting observation in aforementioned simulations of Memmer [13]. It concerns the appearance of a spontaneously chiral, helical state close to the uniaxial nematic-smectic phase transition. Memmer, however, has made it clear that the existence of the helical structure might be an artifact of the method he used for this structure was not reproduced in every run.

The Metropolis MC simulations for model bent-core molecules with dipole moments have also been carried out with an attempt to bringing the molecular modeling close to the experimental situation. Unfortunately, the presence of a single dipole located on the C_2 molecular axis has led so far to neither N_B nor N_U [15,17,18]. But two point dipoles placed at the centers of the lateral sites of a three GB bent-core molecule were shown to stabilize the N_U phase in NPT MC simulations [18]. Moving the dipoles towards the terminal positions of the molecular arms broadened the uniaxial nematic range. Finally, the molecules with terminal flexible chains also do not help to stabilize N_U or N_B [17], but the simultaneous presence of flexible tails and molecular dipoles along the C_2 axis can lead to the N_U phase [17]. However, in none of the off-lattice simulations mentioned so far the biaxial nematic phase was detected.

To date, the only off-lattice simulation for bent-core systems that reveals the biaxial nematic phase has been that of Peláez and Wilson [19]. They performed the Molecular Dynamics simulation for real molecules with experimentally detected N_B phase [2,3] using a full-atomistic potential. The biaxial nematic phase with local ferroelectric domains was observed on cooling down an isotropic phase. However, the same atomistic model with electrostatic charges switched off gave a stable smectic phase instead of N_B. This seems to indicate that a subtle balance between an average bent molecular shape, molecular flexibility and transverse dipoles is essential for bent-core mesogenic molecules to stabilize the N_B phase, and that the question of the minimal molecular features necessary to obtain N_B is still open.

In this work we present results of Metropolis MC NPT simulations aimed at seeking for such minimal molecular features necessary to stabilize N_B for V-shaped molecules. We check as whether the elongation of the molecular arms can play any role. We also study some consequences of fluctuations in opening angle. We choose the model similar to that of Memmer [13], where bent-core molecules were built out of two Gay-Berne (GB) centers representing molecule's arms. An attractive feature of the model [13] is that it shows the stable N_U phase in a relatively wide temperature range. Our model differs from the original one by longer molecular arms. In addition we allow for harmonic fluctuations in the opening angle. Both changes are shown to have a significant effect on the nematic polymorphism, indicating that the lengthening of the molecular arms can help in stabilizing the N_B phase.

The paper is organized as follows. In Section 2 we define model banana-shaped molecules and give some computational details. In Section 3 we introduce relevant order parameters and distribution functions used to identify structures. Results are presented in Section 4 and a short summary is given in Section 5.

2. Model and Computational Details

We define a banana-shaped Gay-Berne molecule by linking two prolate GB molecules, a and b, as shown in Figure 1. The positions of the GB centers are given by vectors $\mathbf{r}_a$ and $\mathbf{r}_b$. In addition, each molecule is parameterized with two internal coordinates: (i) the opening angle γ ($0° < \gamma < 180°$) between the unit vectors $\hat{\mathbf{u}}_a$ and $\hat{\mathbf{u}}_b$ entering definition of the GB potentials and (ii) the shift c of the GB centers along the molecule's arms. We also introducea molecule-fixed orthonormal coordinate system with basis vectors $\{\hat{\mathbf{e}}'_\mu, \mu = 1, 2\}$, where $\hat{\mathbf{e}}'_2$ is taken to belong to the line through endpoints of $\mathbf{r}_a$ and $\mathbf{r}_b$, $\hat{\mathbf{e}}'_1$ is placed along the molecular C_2-axis, parallel to $\hat{\mathbf{u}}_a + \hat{\mathbf{u}}_b$, and $\hat{\mathbf{e}}'_0 = \hat{\mathbf{e}}'_1 \times \hat{\mathbf{e}}'_2$. Details of the parameterization are given in Figure 1.

The intermolecular interaction between a pair (i, j) of the molecules, separated by the intermolecular vector $R_{ij} = \frac{1}{2}\left[\left(\mathbf{r}_a^{(j)} + \mathbf{r}_b^{(j)}\right) - \left(\mathbf{r}_a^{(i)} + \mathbf{r}_b^{(i)}\right)\right]$ is given by:

$$U\left(\left\{\hat{\mathbf{e}}'^{(i)}_\mu\right\}, \left\{\hat{\mathbf{e}}'^{(j)}_\mu\right\}, \gamma_i, \gamma_j, \boldsymbol{R_{ij}}\right) = \sum_{\alpha=a,b} \sum_{\beta=a,b} U_{GB}(\hat{\mathbf{u}}_\alpha^{(i)}, \hat{\mathbf{u}}_\beta^{(j)}, \mathbf{r}_{\alpha\beta}^{(i,j)}) \tag{1}$$

where $\boldsymbol{r}_{\alpha\beta}^{(i,j)} = \boldsymbol{r}_\beta^{(j)} - r_\alpha^{(i)}$ is the intermolecular vector connecting the GB centers α, β(α,β = a, b) of the molecules i and j, respectively, with the vectors $\hat{\boldsymbol{u}}_\alpha^{(i)}, \hat{\boldsymbol{u}}_\beta^{(j)}, \boldsymbol{r}_{\alpha\beta}^{(i,j)}$ expressed through $\{\hat{\mathbf{e}}'^{(i)}_\mu\}, \{\hat{\mathbf{e}}'^{(j)}_\mu\}$, γ_i, γ_j, $\mathbf{R}_{ij}$ and c. Finally, the U_{GB} term is the Gay-Berne interaction [20] between the individual arms α , β of the molecules i and j, respectively. It reads

$$\begin{aligned} U_{GB}(\hat{\boldsymbol{u}}_\alpha^{(\boldsymbol{i})}, \hat{\boldsymbol{u}}_\beta^{(\boldsymbol{j})}, \boldsymbol{r}_{\boldsymbol{\alpha\beta}}^{(\boldsymbol{i,j})}) = 4\epsilon(\hat{\boldsymbol{u}}_\alpha^{(i)}, \hat{\boldsymbol{u}}_\beta^{(j)}, \hat{\boldsymbol{r}}_{\boldsymbol{\alpha\beta}}^{(\boldsymbol{i,j})}) \Bigg[& \left(\frac{\sigma_0}{r_{\alpha\beta}^{(i,j)} - \sigma(\hat{\boldsymbol{u}}_\alpha^{(\boldsymbol{i})}, \hat{\boldsymbol{u}}_\beta^{(\boldsymbol{j})}, \hat{\boldsymbol{r}}_{\boldsymbol{\alpha\beta}}^{(\boldsymbol{i,j})}) + \sigma_0} \right)^{12} \\ & - \left(\frac{\sigma_0}{(r_{\alpha\beta}^{(i,j)} - \sigma(\hat{\boldsymbol{u}}_\alpha^{(\boldsymbol{i})}, \hat{\boldsymbol{u}}_\beta^{(\boldsymbol{j})}, \hat{\boldsymbol{r}}_{\boldsymbol{\alpha\beta}}^{(\boldsymbol{i,j})}) + \sigma_0} \right)^{6} \Bigg] \end{aligned} \tag{2}$$

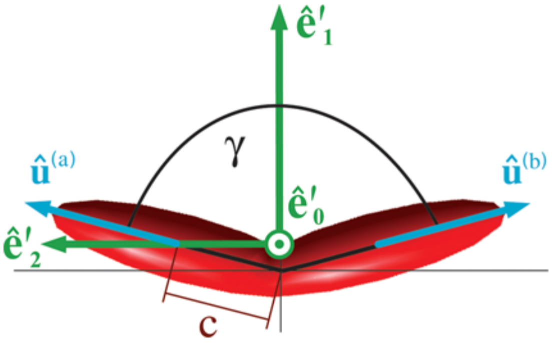

Figure 1. Parameterization of model bent-core molecules used in simulations. (Figure appears in color online.)

where $\hat{\boldsymbol{r}}_{\alpha\beta}^{(i,j)} = \boldsymbol{r}_{\alpha\beta}^{(i,j)}/r_{\alpha\beta}^{(i,j)}$ is the unit vector and $r_{\alpha\beta}^{(i,j)} = \left|\boldsymbol{r}_{\alpha\beta}^{(i,j)}\right|$. The functions $\epsilon(\hat{\boldsymbol{u}}_{\alpha}^{(i)}, \hat{\boldsymbol{u}}_{\beta}^{(j)}, \hat{\boldsymbol{r}}_{\alpha\beta}^{(i,j)})$ and $\sigma(\hat{\boldsymbol{u}}_{\alpha}^{(i)}, \hat{\boldsymbol{u}}_{\beta}^{(j)}, \hat{\boldsymbol{r}}_{\alpha\beta}^{(i,j)})$ depend on four GB parameters κ, κ', μ and ν and their explicit form is found in [20]. In addition, each molecule i is allowed to vary its opening angle γ_i about γ_0 with a harmonic contribution to the potential energy

$$U_{int}^{(i)} = \begin{cases} \infty & if|\gamma_i - \gamma_0| > \gamma_{max} \\ k(\gamma_i - \gamma_0)^2 & othervise \end{cases} \tag{3}$$

where k is the harmonic constant, γ_0 is the angle for which internal energy has a minimum and γ_{max} is the angle of maximal deflection. The case of $k = \infty$ corresponds to a rigid molecule.

In our simulations we study the model with the following GB parameters: $\kappa = 4$, $\kappa' = 5.0$, $\mu = 1$ and $\nu = 2$. In addition we assume $\gamma_0 = 140°$, $\gamma_{max} = 38°$, $k = 25$, ∞ and $c = 1.7$, where c is chosen such that a smooth molecular shape is obtained for opening angles in the range studied $(102° - 178°)$. Finally, throughout the paper angles are expressed in degrees and all other parameters are rendered dimensionless. Their definitions are found *e.g.,* in [13].

Memmer [13] carried out MC simulations for a similar model, but with shorter molecular arms. The parameters different from ours were $\kappa = 3$ and $c = 1$. Only the case with rigid molecules ($k = \infty$) was considered. Thus, a comparison of our results with those of Memmer [13] will allow us to look at the influence of the arms' elongation and of the molecular arms fluctuations on the nematic polymorphism.

All simulations are performed using Metropolis MC simulations in NPT ensemble [21]. The system consists of $N = 1088$ molecules placed in a rectangular box with periodic boundary conditions and the nearest image convention taken regard of. A sequence of configurational states is generated according to the probability density

$$f(\Gamma, \Omega, \Phi) = \frac{\prod_{i=1}^{N} \sqrt{(1 + 3\cos^2(\frac{\gamma_i}{2}))(1 - \cos^2(\frac{\gamma_i}{2}))\cos^2(\frac{\gamma_i}{2})(4 - 3\cos^2(\frac{\gamma_i}{2}))} \; \exp[-\frac{U_{total}(\Gamma, \Omega, \Phi) + PV - NTln(V)}{T}]}{Z'_{NPT}}, \tag{4}$$

where Γ, Ω, Φ denote respectively positions, orientations and opening angles of all molecules, V is the volume of the system, U_{total} represents the total potential energy and Z'_{NPT} denotes the partition function. Boltzmann constant, not present in Eq.(4), is included into definition of the reduced temperature T. The formula (4) for the probability density contains square root factors coming from the integration over momenta. For rigid molecules the square root part gives a constant factor and, hence, cancels out with similar terms in Z'_{NPT}.

The MC cycle consisted of probing a new configuration for each molecule followed by volume rescaling along a randomly chosen edge of the simulation box. A trial molecularconfiguration was generated by a random move of the molecule's center of mass, a random rotation about randomly chosen axis out of the laboratory reference system, a flip of the steric dipole, and a random change of the opening angle. In simulations $10\% - 50\%$ of new molecular configurations and $10\% - 60\%$ of system rescalings were accepted. The lower acceptance ratios were used for dense, highly ordered states, allowing to partly overcome the metastability traps. Simulations were carried out under the pressure of $P = 3$ and with spherical cutoff for the GB potential at the distance $\boldsymbol{r}_{\alpha\beta}^{(i,j)} = 5.0$. The pressure was taken the same as in [13]. Simulations were initialized in the isotropic liquid and the temperature was lowered in adjustable steps until transition into a highly ordered crystalline smectic phase took place. In addition, the crystalline phase found on cooling was heated up all the way back to estimate the stability range of the phases found. The equilibration appeared slow and took between 5×10^5 and 10^6 cycles after which the data were collected for structure analysis once per 10 cycles over a production run of 10^4 cycles.

Interestingly, the biaxial nematic phase was found on cooling down. To check its stability we also melted ground state crystalline structures under higher pressures, from $P = 4$ to $P = 10$ in step of 1.

3. Order Parameters and Distribution Functions

In order to characterize the long-range orientational order of the molecules the alignment tensors were utilized. They are given by

$$Q_{\mu\nu}^{\eta} = \frac{1}{2N} \langle \sum_{i=1}^{N} (3 l_{\eta\mu}^{(i)} l_{\eta\nu}^{(i)} - \delta_{\mu\nu}) \rangle \tag{5}$$

where $l_{\eta\mu}^{(i)} = \hat{\boldsymbol{e}}_{\eta}^{\prime(i)} \cdot \hat{\boldsymbol{e}}_{\mu}$, and $\{\hat{\boldsymbol{e}}_{\mu}\}$ constitute a base of the laboratory reference system (η, µ, $\nu \in \{0,1,2\}$). Eigenvectors of $Q_{\mu\nu}^{\eta}$ correspond to the directors of the phase and the associated eigenvalues are the orientational order parameters measured with respect to these directors. For isotropic phase all eigenvalues of each tensor $Q_{\mu\nu}^{\eta}$ vanish. For uniaxial phase each tensor $Q_{\mu\nu}^{\eta}$ has one eigenvalue different than the other two, which are equal to each other. In case of the biaxial phase all eigenvalues of $Q_{\mu\nu}^{\eta}$ are, in general, different. However, it might happen that one of the tensors be uniaxial [22].

The presence of smectic order was detected by means of the one-particle distribution function $P^{(1)}$, calculated along the main director. More specifically, let the director $\hat{\boldsymbol{n}}$, corresponding to the largest eigenvalue of $Q_{\mu\nu}^{2}$ be parallel to $\hat{\boldsymbol{e}}_2$. Then the smectic ordering along $\hat{\boldsymbol{n}}$ can be examined with the distribution function

$$P^{(1)}(z) = \frac{\overline{L_z}}{N} \langle \sum_{i=1}^{N} \delta(z - Z_i) \rangle, \tag{6}$$

where $\overline{L_z}$ is the average length of the simulation box along $\hat{\boldsymbol{e}}_2$, Z_i represents coordinate of the i-th molecule along $\hat{\boldsymbol{e}}_2$, and δ is the Dirac delta.

The in-layer structure of the smectic layers was examined with the two-point transverse correlation function

$$g_{\perp}^{(2)}(r_{\perp}) = \frac{\bar{V}}{4\pi r_{\perp} D N^2} \langle \sum_{i} \sum_{j \neq i} \delta(r_{\perp} - |R_i - R_j|_{\perp}) \Theta(D - |Z_i - Z_j|) \rangle \tag{7}$$

where $D = 0.5$ is the thickness of the slice within which correlations were calculated, $\bar{V}$ is the average volume of the simulation box, and $|\boldsymbol{R_i} - \boldsymbol{R_j}|_{\perp}$ is the projection of the vector linking the origins *i, j* of the molecule-fixed reference frames on a surface perpendicular to $\hat{n}$. Owing the small system size we were unable to distinguish between hexatic- and crystalline orders and, for this reason, a phase with long-range hexagonal order within layers is referred to as a crystal.

For flexible molecules the one-particle distribution function of opening angles was definedas:

$$P^{(1)}(\gamma) = \frac{\pi}{N}\langle\sum_{i=1}^{N}\delta(\gamma-\gamma_i)\rangle. \tag{8}$$

Finally, the relative stability range for a given phase f was examined by calculating the coefficients

$$\Delta T^f = (T_H^f - T_L^f)/T_L^f \tag{9}$$

$$\Delta\rho^f = (\rho_H^f - \rho_L^f)/\rho_H^f \tag{10}$$

where $T_H^f(\varrho_H^f)$, $T_L^f(\varrho_L^f)$ represent upper and lower limit, respectively, of temperature (density), for which the phase f is detected.

4. Results and Discussion

Cooling down the system of rigid molecules below $T \cong 4.1$ leads to a phase transition from isotropic liquid to uniaxial nematic (Fig. 2,3). Further lowering of the temperature causes stabilization of the biaxial nematic phase, which is found for $2.7 < T < 3.0$ (Fig. 2,3). Periodic modulation of $P^{(1)}(z)$ (Fig. 3) emerges only below $T \cong 2.8$, but for $2.7 \lesssim T \lesssim 2.8$ this modulation is highly irregular, with amplitude not exceeding 0.2. Distinguishable smectic order is present only from below $T \cong 2.6$ and is accompanied by the hexagonal long-range order within smectic layers (see $g_\perp^2(r_\perp)$ shown in Fig. 3). The phase is antiferroelectric with respect to the steric dipoles (Fig. 4). As we cannot distinguish between hexatic and crystalline order we classify this phase as a biaxial, hexagonal and antiferroelectric crystal.The crystal melts into uniaxial nematic at $T \cong 3.2$. On cooling down the biaxial nematic appears below $T \cong 3.2$; hence without a credible calculation of the free energy it is not possible to settle if N_B is really absolutely stable in our simulations (Fig. 2,5). Studies at higher pressures also do not resolve this issue unambiguously. However, owing that the hysteresis affects both measurements it is quite likely that the biaxial nematic might be absolutely stable in a small temperature interval. Further increase of temperature transforms uniaxial nematic into isotropic liquid what takes place at $T \cong 4.4$. The coexistence temperature of isotropic liquid and uniaxial nematic is pinpointed by localizing the discontinuity in the density between these phases (Fig. 5), which yields $T \cong 4.2$.

For the model bent-core molecules with shorter arms of $\kappa = 3.0$ [13] no evidence of the biaxial nematic phase was reported. Thus we conclude that molecules with more elongated arms should help in stabilizing N_B. In addition, for Memmer's model $\Delta T^N \cong 0.5$ and $\Delta\rho^N \cong 0.118$ while the same coefficients for our model are $\Delta T^N \cong 0.313$ and $\Delta\rho^N \cong 0.127$. That is the elongation of the arms enhances the density

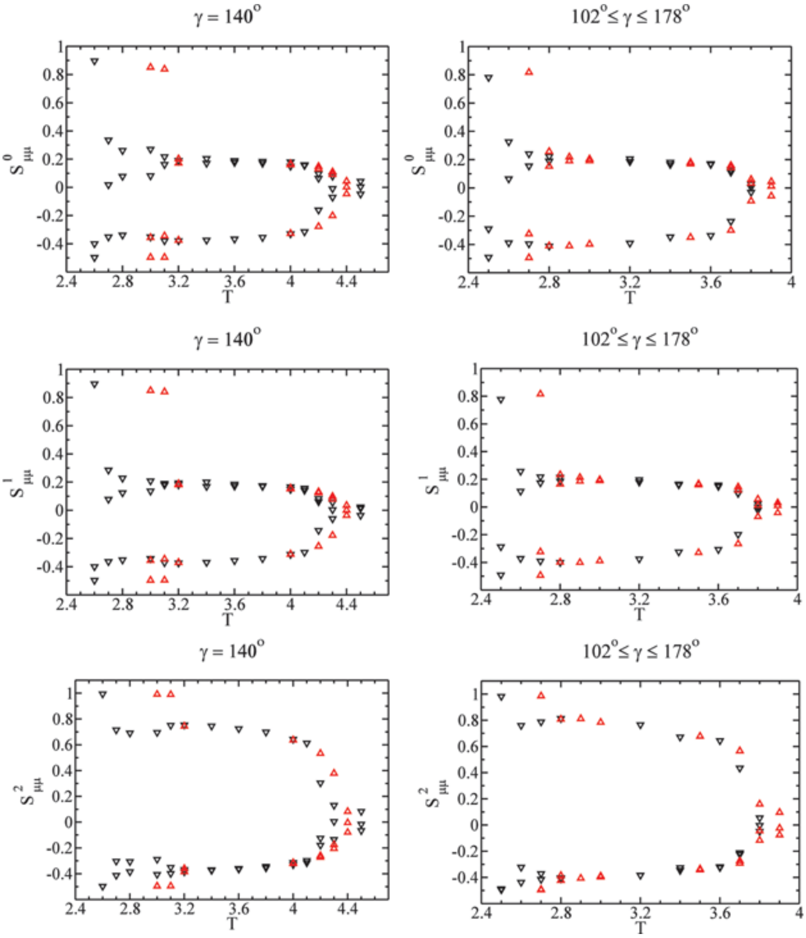

Figure 2. Eigenvalues $S^{\delta}_{\mu\mu}$ of tensors $Q^{\delta}_{\mu\nu}$for system of rigid ($\gamma = 140°$) and flexible ($102° \leq \gamma \leq 178°$) molecules obtained on cooling down (∇) and heating up (Δ) the system. The identified phases are a) orientationally isotropic, when eigenvalues of $Q^{\delta}_{\mu\nu}$ are close to zero; b) uniaxial, when each tensor $Q^{\delta}_{\mu\nu}$ has only two different eigenvalues; c) biaxial, when at least two tensors $Q^{\delta}_{\mu\nu}$ have all three eigenvalues different. Note that the biaxial nematic phase appears when the system is cooled down. (Figure appears in color online.)

range for which nematic phases can be stable. Finally, in [13] a helical structure between uniaxial nematic and smectic has been reported. Simulations we carried out do not show a formation of any helical order.

Cooling down the system of the flexible bent-core molecules leads to the following phase transitions: at $T \cong 3.7$ the isotropic liquid transforms into the uniaxial nematic and at $T \cong 2.7$ the nematic phase becomes biaxial (Fig. 2,3). For $T \cong 2.6$ the one-particle distribution function, $P^{(1)}(z)$, develops an irregular modulation of magnitude smaller than 0.2. The ordering becomes periodic along the director for $T \lesssim 2.5$ which is attributed to the formation of smectic layers. Within the layers the molecules form again a hexagonal lattice, Figure 3, with snapshots being similar to the one shown in Figure 4. Hence, the phase can again be classified as biaxial, hexagonal and antiferroelectric crystal.

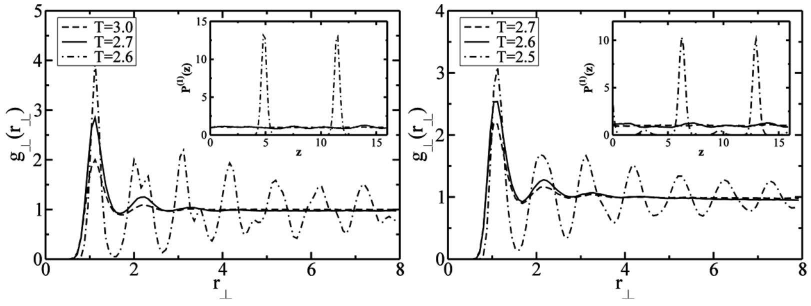

Figure 3. Functions $g_{\perp}^{(2)}(r_{\perp})$ and $P^{(1)}(z)$ obtained on cooling for the system of rigid (left) and flexible (right) molecules. For $T \leq 2.7$ (left) and for $T \leq 2.6$ (right) the system gains smectic order with hexagonal long-range order within layers.

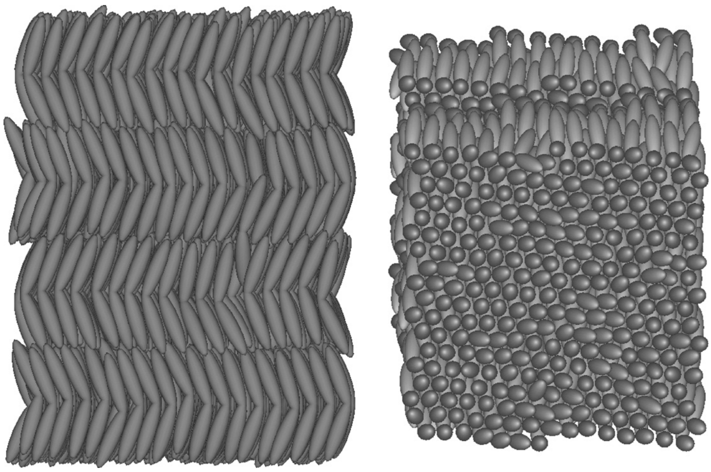

Figure 4. Left: side view of the crystalline phase obtained for the rigid model at $T = 2.6$. Steric dipoles within neighboring layers have opposite orientations making the crystalline structure "antiferroelectric". Right: top view of hexagonal long-range order within smectic layers.

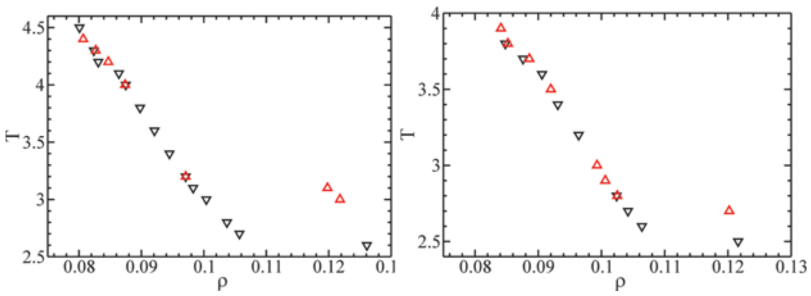

Figure 5. Relation between density and temperature obtained for the system of rigid (left) and flexible (right) molecules on cooling down (∇) and heating up (Δ). At $T \cong 4.2$ (left) and $T \cong 3.7$ (right) isotropic liquid coexists with uniaxial nematic. Hysteresis between liquid crystalline and crystalline phases for $T \leq 3.2$ (left) and $T \leq 2.8$ (right) is also shown. (Figure appears in color online.)

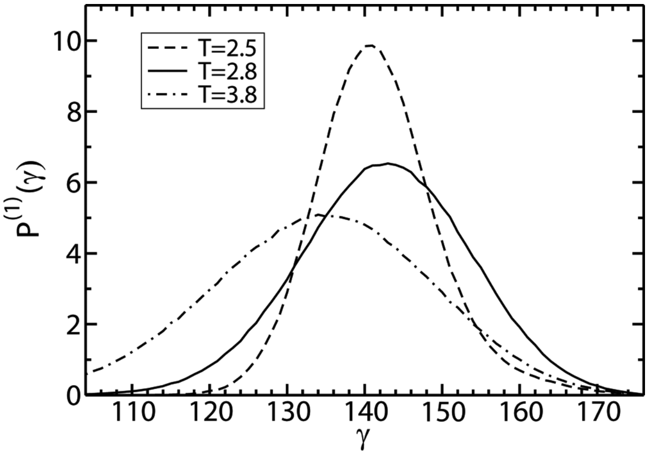

Figure 6. Distribution of opening angles $P^{(1)}(\gamma)$ for system of flexible molecules.

The crystalline phase of the model melts directly into the uniaxial nematic phase at $T \cong 2.8$ and, subsequently, the uniaxial nematic transforms into an isotropic liquid at $T \cong 3.8$. From Figure 5 we can estimate that the uniaxial nematic and the isotropic liquid coexist at $T \approx 3.7$. Like for the rigid model the presence of hysteresis (Fig. 2,5) does not allow to settle as whether the biaxial nematic is absolutely stable. Note, however, that fluctuations in the opening angle seem to have a destabilizing effect on the biaxial nematic phase observed on cooling, Figure 2.

For the model with flexible molecules the average opening angle, $\bar{\gamma}$, changes with temperature (Fig. 6). At low temperatures, in the crystalline phase, $\bar{\gamma}$ does not differ much from γ_0 (*i.e.,* $\bar{\gamma} \cong 140.5°$ for $T=2.5$). As temperature increases the average opening angle first increases to $\bar{\gamma} \cong 143°$ in the uniaxial nematic phase ($T=2.8$) to next decrease to $\bar{\gamma} \cong 135°$ in the isotropic liquid phase ($T=3.8$).

The observation of N_B on cooling encouraged us to perform additional simulations at higher pressures. In these simulations we limited ourselves to the rigid model of $\gamma_0 = 140°$ and to integer values of pressure ranging from 4 to 14. In addition, we carried out the simulations along the $P=10$ isobar for opening angles of 125°, 130° and 135°. In all cases we melted the ground state configurations and sought for an interval of stable biaxial nematic phase. Apart from the model with the opening angle of 125°, the ground state crystalline structures melted directly to the uniaxial nematic phase. For the opening angle of 125° we observed a direct melting to the isotropic liquid phase. As a result we cannot confirm that the biaxial nematic found on cooling is absolutely stable.

5. Conclusion

This paper contains results of MC NPT simulations performed for the system of model bent-core particles. The arms of V-shaped molecules were built out of two Gay-Berne sites. Two variants of the model were studied, with rigid- and with fluctuating angle between the arms. For both models decrease of temperature leads to the sequence of phases: isotropic liquid, uniaxial nematic, biaxial nematic and biaxial antiferroelectric hexagonal crystal. On heating the ground state configuration the biaxial nematic is superseded by a metastable crystalline phase. However, in contrast to the model with molecules of shorter arms ($\kappa = 3.0$) [13], the present systems, especially the rigid one, clearly show a tendency to stabilize N_B (for some simpler systems with generic N_B phase see *e.g.,* [22–26]). In addition, the V-shaped molecules with longer arms extend the range of density in which the nematic polymorphism can be present. Finally, the helical structure found in [13] was not detected in the present simulations.

Acknowledgment

This work is supported in part by the International PhD Projects Programme of the Foundation for Polish Science within the European Regional Development Fund of the European Union, agreement no. MPD/2009/6.

References

[1] Takezoe, H., & Takanishi, Y. (2006). *Jap. J. Appl. Phys.*, *45*, 597.

[2] Madsen, L. A., Dingemans, T. J., Nakata, M., & Samulski, E. T. (2004). *Phys. Rev. Lett.*, *92*, 145505.

[3] Acharya, B. R., Primak, A., & Kumar, S. (2004). *Phys. Rev. Lett.*, *92*, 145506.

[4] Prasad, V., Kang, S. W., Suresh, K. A., Joshi, L., Wang, Q., & Kumar, S. (2005). *J. Am. Chem. Soc.*, *127*, 17224.

[5] Lehmann, M., Kang, S. W., Koehn, C., Haseloh, S., Kolb, U., Schollmeyer, D., Wang, Q. B., & Kumar, S. (2006). *J. Mater. Chem.*, *16*, 4326.

[6] Luckhurst, G. R. (2004). *Nature*, *430*, 413.

[7] Berardi, R., Muccioli, L., Orlandi, S., Ricci, M., & Zannoni, C. (2008). *J. Phys. Condens. Matter*, *20*, 463101.

[8] Bates, M. A., & Luckhurst, G. R. (2005). *Phys. Rev., E 72*, 51702.

[9] Bates, M. A. (2006). *Phys. Rev. E*, *74*, 61702.

[10] Bates, M. A. (2007). *Chem. Phys. Lett.*, *437*, 189.

[11] Camp, P. J., Allen, M. P., & Masters, A. J. (1999). *J. Chem. Phys.*, *111*, 9871.

[12] Lansac, Y., Maiti, P. K., Clark, N. A., & Glaser, M. A. (2003). *Phys. Rev. E*, *67*, 011703.

[13] Memmer, R. (2002). *Liq. Cryst.*, *29*, 483.

[14] Johnston, S. J., Low, R. J., & Neal, M. P. (2002). *Phys. Rev., E*, *65*, 051706.

[15] Johnston, S. J., Low, R. J., & Neal, M. P. (2002). *Phys. Rev. E*, *66*, 061702.

[16] Dewar, A., & Camp, P. J. (2004). *Phys. Rev. E*, *70*, 011704.

[17] Dewar, A., & Camp, P. J. (2005). *J. Chem. Phys.*, *123*, 174907.

[18] Orlandi, S., Berardi, R.,Stelzer,J., & Zannoni, C. (2006). *J. Chem. Phys.*, *124*, 124907.

[19] Peláez, J., & Wilson, M. R. (2006). *Phys. Rev. Lett.*, *97*, 267801.

[20] Gay, J. G., & Berne, B. J. (1981). *J. Chem. Phys.*, *74*, 3316.

[21] Allen, M. P., & Tildesley, D. J. (1987). *Computer Simulation of Liquids*, Clarendon Press: Oxford.

[22] Gramsbergen, E. F., Longa, L., & de Jeu, W. H. (1986). *Phys. Rep.*, *135*, 195.

[23] Allender, D., & Longa, L. (2008). *Phys. Rev. E*, *78*, 011704.

[24] Longa, L., Grzybowski, P., Romano, S., & Virga, E. (2005). *Phys. Rev. E*, *71*, 051714.

[25] Longa, L., Pająk, G., & Wydro, T. (2009). *Phys. Rev., E*, *79*, 040701 (R).

[26] Longa, L., Pająk, G., & Wydro, T. (2007). *Phys.Rev., E*, *76*, 011703.